Abdominal Imaging

Published online: 7 June 2013

Abdom Imaging (2013) 38:1277–1285
DOI: 10.1007/s00261-013-0016-6

Hepatic pseudolymphoma: imaging–pathologic correlation with special reference to hemodynamic analysis

Kotaro Yoshida, Satoshi Kobayashi, Osamu Matsui, Toshifumi Gabata, Junichiro Sanada, Wataru Koda, Tetsuya Minami, Yasuji Ryu, Kazuto Kozaka, Azusa Kitao

Department of Radiology, Kanazawa University School of Medicine, 13-1, Takara-Machi, Kanazawa 920-8641, Japan

Abstract

Objectives: To clarify radiological findings and hemodynamic characteristics of hepatic pseudolymphoma, as compared with the histopathological findings.
Methods: Radiological findings of ten histopathologically confirmed hepatic pseudolymphomas in seven patients were examined using US, CT, and MRI. Six patients also underwent angiography-assisted CT, including CT during arterial portography (CTAP) and CT during hepatic arteriography (CTHA) to analyze hemodynamics.
Results: The nodules were depicted as hypoechoic on US, hypodense on precontrast CT, hypointense on T1-weighted images, and hyperintense on T2-weighted images. On contrast-enhanced CT/MRI, they showed various degrees of enhancement, and sometimes, perinodular enhancement was observed at the arterial dominant and/or equilibrium phase. On CTAP, the nodules showed portal perfusion defects, including some in the perinodular liver parenchyma. On CTHA, irregular bordered enhancement was observed in perinodular liver parenchyma on early phase, and continued until delayed phase. Some nodules had preserved intra-tumoral portal tracts. Histopathologically, the nodules consisted of marked lymphoid cells. In perinodular liver parenchyma, stenosis or disappearance of portal venules, caused by lymphoid cell infiltration in the portal tracts, was observed.
Conclusions: Hepatic pseudolymphoma showed some characteristic radiological findings including hemodynamics on CT, MRI, and angiography-assisted CT. These findings are useful in the differentiation from hepatocellular carcinoma and other tumors.

Key words: Hepatic pseudolymphoma—Reactive lymphoid hyperplasia—Nodular lymphoid hyperplasia—Perinodular enhancement—CTHA

Abbreviations

CTHA	CT during hepatic arteriography
CTAP	CT during arterial portography
SLD-CTHA	Single-level dynamic CT during hepatic arteriography

Hepatic pseudolymphoma, also known as reactive lymphoid hyperplasia and nodular lymphoid hyperplasia, is a rare hepatic nodular lesion [1]. It exhibits unique histopathological findings characterized by marked proliferation of lymphocytes forming follicles with germinal centers [2–4]. Although the number of reported cases of hepatic pseudolymphoma has increased, no multi-case study focusing on the radiological findings has been reported, and it is believed to be difficult to diagnose without needle biopsy or surgical resection [5, 6]. We have experienced several cases of histopathologically confirmed hepatic pseudolymphoma examined with various radiological modalities including ultrasonography (US), CT, and MRI. Five nodules were diagnosed with percutaneous core needle biopsy specimens and regressed without any treatment, and the other five with resected specimens. Moreover, we analyzed the hemodynamics of hepatic pseudolymphomas with angiography-assisted CT such as CT during arterial portography

Correspondence to: Kotaro Yoshida; *email:* kotaroy@med.kanazawa-u.ac.jp

Table 1. The clinical features of patients examined in this study

Patient	Sex	Age (years)	Past history	Location	Size (mm)	Number of the lesions	Diagnostic procedure
1	Female	58	None	S7	10	1	Resection
2	Female	63	PBC	S7	13	2	Resection
				S6	6		Resection
3	Female	43	Breast cancer	S3	13	8	Resection
				S6	8		Resection
4	Male	81	None	S2	55	1	Biopsy
5	Female	73	None	S2	45	8	Biopsy
6	Female	64	APS, Takayasu's arteritis	S6	19	2	Biopsy
7	Male	54	Follicular lymphoma of the duodenum	S8	44	2	Biopsy
				S4	29		Biopsy

PBC, primary biliary cirrhosis; *APS*, antiphospholipid syndrome

(CTAP) and CT during hepatic arteriography (CTHA). This study was undertaken to clarify the radiological findings of hepatic pseudolymphoma including its hemodynamic characteristics as compared with the histopathological findings.

Materials and methods

Patients

From the pathological files of our institution, we identified ten histopathologically confirmed hepatic pseudolymphomas in seven patients. Clinical features of the seven patients are listed in Table 1. Five patients were female, and two male (range 43–81 years, mean age 62.3). The clinico-pathological features of three patients (patient 2, 4, 6) were previously reported [7, 8]. Five nodules were diagnosed with resected specimens, and the other five with percutaneous core needle biopsy specimens. Five patients had multiple lesions, and the other two had a single lesion. The lesions ranged from 0.6 to 5.5 cm (mean, 2.4 cm) in diameter. One pseudolymphoma coexisted with primary biliary cirrhosis, another with follicular lymphoma of the duodenum, and another with antiphospholipid syndrome and Takayasu's arteritis. One patient had undergone operation for breast cancer 16 years previously. Three patients did not have any liver disease or past history of other diseases. All patients were asymptomatic, and the hepatic lesions were incidentally detected by US or CT. Various tumor markers including alpha-fetoprotein, des-gamma-carboxy prothrombin, and serum-soluble interleukin-2 receptor were negative in all cases.

Images

Six of seven patients were examined with US. For all seven patients, contrast-enhanced CT and MRI were also performed. Six patients were examined with multi-phasic contrast-enhanced CT using a multidetector row CT system (LightSpeed Plus or Ultra16 or VCT, General Electric Medical Systems, Milwaukee, WI) and one patient underwent CT examination using a single-detector row CT (HiSpeed Advantage, General Electric Medical Systems Milwaukee, WI). MRI was performed on a 1.5- or 3.0-T superconductor unit (Signa Horizon or Signa HDx, GE Healthcare, Milwaukee, WI). Spin-echo T1-weighted images and fast spin-echo T2-weighted images with fat saturation and gadolinium (Gd) or gadolinium ethoxybenzyl diethylenetriamine pentaacetic acid (Gd-EOB-DTPA)-enhanced dynamic MRI were obtained from all patients. Diffusion-weighted images (DWI) were obtained from four patients. Three patients were examined with superparamagnetic iron oxide (SPIO)-enhanced T2-weighted images, and six with Gd-EOB-DTPA-enhanced T1-weighted images (hepatobiliary phase). The details of the imaging sequences, contrast medium (concentration, total injected volume, injection speed, etc.), and slice thickness differed between the CT and MRI machines.

Angiography-assisted CT images

For six of seven patients, angiography was performed, for which written informed consent had been obtained before the examination. Furthermore, angiography-assisted CT was performed for analysis of the hemodynamic characteristics of the lesions. CTAP and CTHA were performed after hepatic angiography using Xvision/SP or Aquillion64 (Toshiba Medical Systems, Tokyo, Japan). In one case, CTAP was omitted. After femoral artery puncture, a 4-F catheter was selectively placed in the superior mesenteric artery for scanning CTAP and in the common or proper hepatic artery for scanning CTHA. CTAP scans were obtained at 5–7 mm thick sections, 5–7 mm collimation, 2.5 mm reconstruction intervals, covering the entire liver in a single breath-hold. Helical CT scanning began 25 s after the beginning of the infusion of 50–70 mL iohexol (320–350 mgI/mL, Omnipaque; Daiichi Sankyo, Tokyo, Japan) at a rate of 1.8 mL/s with a power injector. To increase the blood flow and decrease the laminar flow of the portal vein, 5 mg of prostaglandin E1 (Palux; Taisho, Tokyo, Japan)

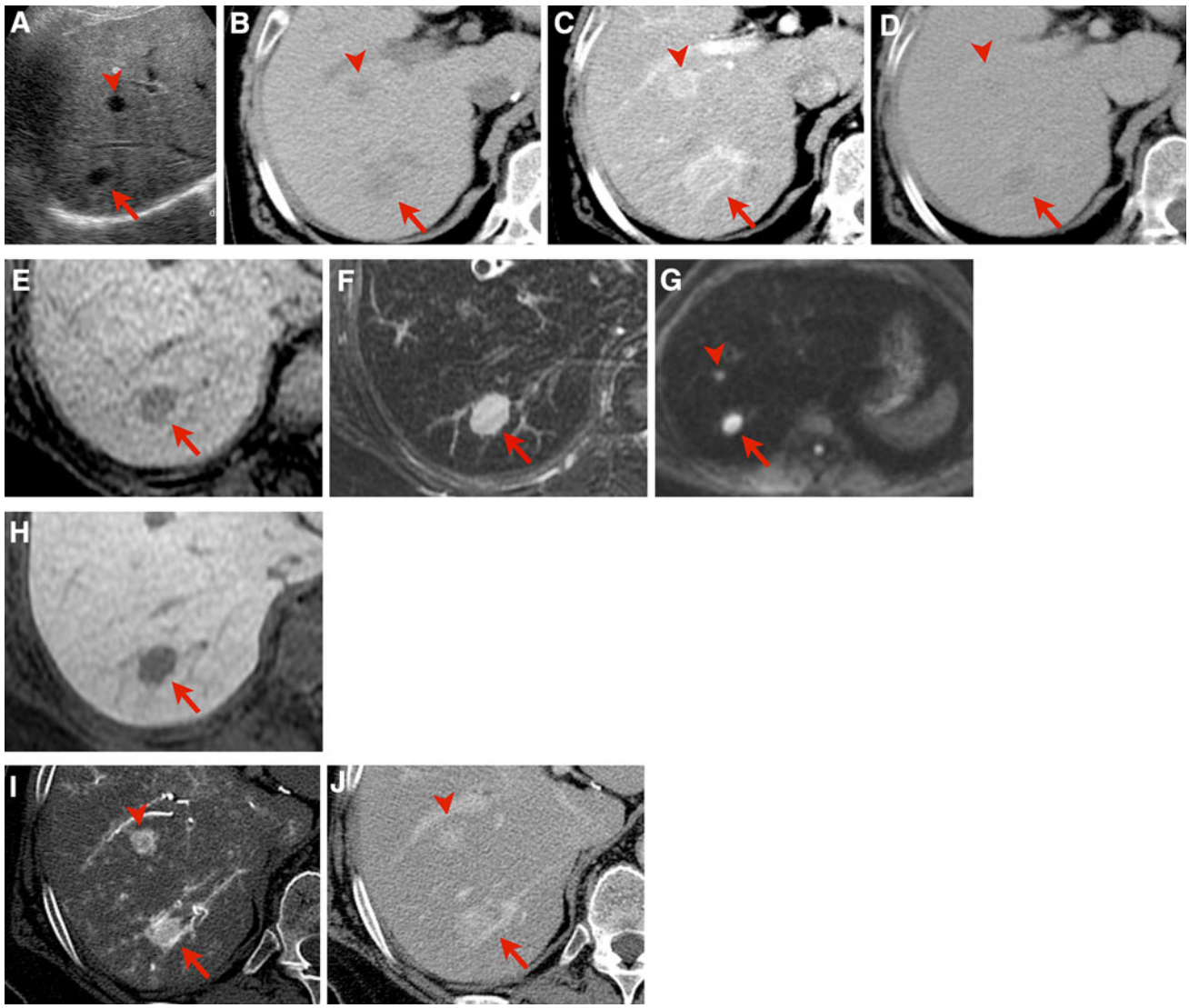

Fig. 1. A 64-year-old woman with pseudolymphomas in segment VII and V of the liver (patient 6). **A** Ultrasound shows a markedly hypoechoic nodule 15 mm in diameter in segment VII (*arrow*). **B–D** Precontrast CT (**B**) shows it as a slightly hypodense mass (*arrow*). On the arterial dominant phase of multi-phasic CT (**C**), this mass demonstrates homogeneous enhancement with dense irregular perinodular enhancement (*arrow*). Equilibrium phase of multi-phasic CT (**D**) shows it as a hypodense mass with slight perinodular enhancement (*arrow*). **E–H** On MRI, T1-weighted image (**E**) shows it as hypointense (*arrow*), T2-weighted image (**F**) as hyperintense (*arrow*), diffusion-weighted image (**G**) as hyperintense (*arrow*), and T1-weighted image of hepatobiliary phase of Gd-EOB-DTPA-enhanced MRI (**H**) as markedly hypointense (*arrow*). **I**, **J** CT during hepatic arteriography (CTHA) shows it as a hypervascular mass with irregularly bordered perinodular enhancement on the early phase (**I**) *arrow*), and prolonged enhancement with perinodular hyperdensity on the delayed phase (**J**, *arrow*). Another nodule in segment V shows similar imaging findings (*arrowheads*).

was injected into the superior mesenteric artery before contrast material infusion. Approximately 10 min after CTAP was performed, CTHA scans were obtained at 3–5 mm thick sections, 3–5 mm collimation, and 1.5–2.5 mm reconstruction intervals. CTHA scanning began 7 s (early phase) and 60 s (delayed phase) after the start of the injection of iohexol into the common/proper hepatic artery at a rate of 1.8 mL/s. The infusion was continued throughout the early phase scanning. In order to assess further the radiological characteristics and hemodynamics of the lesion, single-level dynamic CT during hepatic arteriography (SLD-CTHA) was performed in four patients. Details of the SLD-CTHA method are as follows. Ten milliliters of contrast material was infused at the rate of 1.0 mL/s into the common hepatic artery using a power injector. Scanning began immediately prior to dye injection and was performed without table feed on 3-mm slices during a single

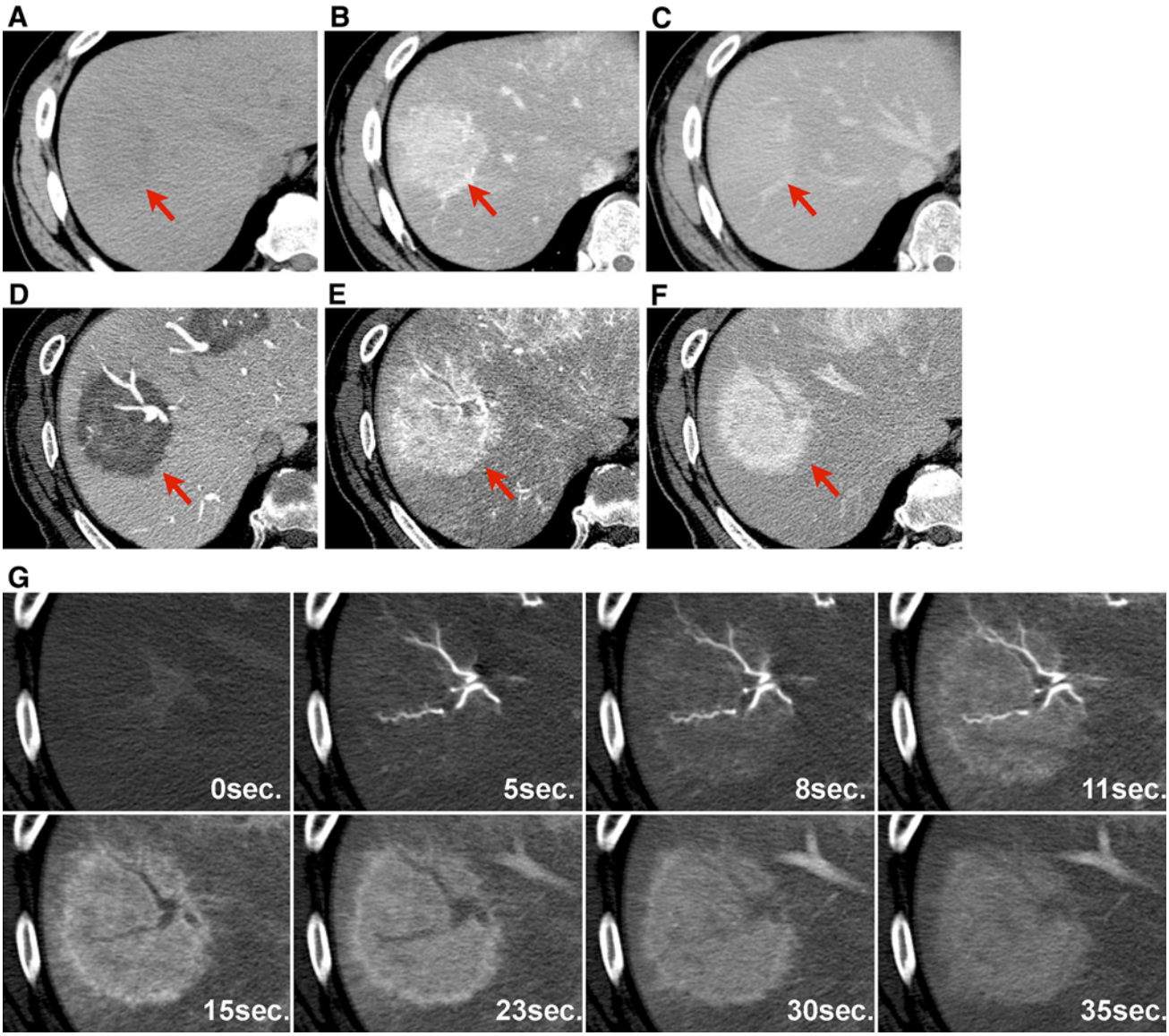

Fig. 2. A 54-year-old woman with pseudolymphomas in segment VIII and VI of the liver (patient 6). **A**–**C** The nodule shows slight hypodensity on precontrast CT (**A**, *arrow*), irregularly bordered but homogeneous internal enhancement and internal portal tracts including hepatic arteries and portal veins on the arterial dominant phase of dynamic CT (**B**, *arrow*), and homogeneous iso or slight hyperdensity on the equilibrium phase (**C**, *arrow*). **D**–**F** The nodule shows definite hypodensity indicating portal perfusion defect and penetrating portal veins in the marginal portion of the nodule on CT during arterial portography (CTAP) (**D**, *arrow*). On CTHA, it shows homogeneous arterial enhancement with irregularly bordered perinodular enhancement on early phase (**E**, *arrow*), and prolonged intranodular and perinodular enhancement on delayed phase (**F**, *arrow*). Note that normal triad (hepatic artery and portal vein) was observed in the tumor without encasement (**D**, **E**). **G** On single-level-dynamic CTHA, the tumor and perinodular liver parenchyma are well opacified by 10–15 s after the beginning of the infusion of contrast medium. Then the enhancement of the tumor gradually diminished and prolonged enhancement of perinodular liver parenchyma was observed at 30–35 s.

breath-hold using a 40-s continuous technique (220 mA, 120 kVp). High-resolution images of the lesions were reconstructed at 1-s intervals using a small FOV. Angiographic procedures were performed by radiologists who each had more than 8 years of experience performing abdominal angiography.

Results

Two cases are shown in Figures 1 and 2. Of all ten nodules, the smallest (in patient 2) was not detected by US, contrast-enhanced CT, or Gd-enhanced dynamic MRI, but was detected by SPIO-enhanced MRI and

angiography-assisted CT images, and resected under intraoperative US guidance.

US findings

On US, all seven detected nodules (100%) were shown as markedly hypoechoic lesions mimicking cysts but without posterior acoustic enhancement. Internal echogenicity of the nodules was homogeneous (Fig. 1A).

CT findings

On precontrast CT, all nine nodules (100%) demonstrated slight hypodensity (Figs. 1B, 2A). On multiphasic CT, six of nine nodules (67%) demonstrated early enhancement (Figs. 1C, 2B) and other three nodules (33%) isodensity on arterial dominant phase images. Nine nodules showed various densities on equilibrium phase images, such as hypodensity in seven nodules (78%) and hyperdensity in two (22%) (Figs. 1D, 2C). When focusing on perinodular liver parenchyma, moreover, irregularly shaped perinodular enhancement was observed in five of nine nodules (56%) on arterial dominant phase images, and in four of nine nodules (44%) on equilibrium phase images (Figs. 1C, D, 2B). Four nodules larger than 2.5 cm in diameter showed homogeneous internal density on each phase, and in two nodules intratumoral portal tracts were identified on arterial dominant phase images.

MRI findings

Nine of nine (100%) nodules detected on MR T1-weighted images showed hypointensity (Fig. 1E). On T2-weighted images, all nine nodules showed hyperintensity (Fig. 1F). On four larger nodules, the intra-tumoral character showed homogeneous intensity on both T1- and T2-weighted images. On DWI, all six nodules in four patients showed restricted diffusion (Fig. 1G). On multiphasic MRI, nine nodules showed various densities such as hyperintensity in seven nodules (78%), isointensity in one (11%), and hypointensity in one (11%) on arterial dominant phase images. On delayed phase images, all nine nodules showed hypointensity (100%). Focusing on the perinodular area, irregularly bordered perinodular enhancement was observed on six of nine (67%) nodules on arterial dominant phase images, and on three of nine (33%) on equilibrium phase images. On SPIO-enhanced T2-weighted images, all three nodules (100%) in two patients demonstrated marked hyperintensity. On T1-weighted images of the hepatobiliary phase of Gd-EOB-DTPA-enhanced MRI, all six nodules (100%) showed marked hypointensity as compared with hyperintense normal liver parenchyma (Fig. 1H).

Angiography-assisted CT findings

On CTAP, all seven nodules showed portal perfusion defects (Fig. 2D). Perinodular liver parenchyma, where the irregular enhancement was observed on contrast-enhanced CT/MRI, also showed portal perfusion defects. This makes the portal perfusion defect area appear a little larger as compared to the true nodular size observed on non-enhanced CT or MRI. On early phase images of CTHA, seven of eight nodules showed hyperdensity, and one isodensity. In all cases, perinodular liver parenchyma showed irregular bordered enhancement compared with the background hepatic parenchyma (Figs. 1I, 2E). On delayed phase images of CTHA, the nodules showed slight hyperdensity or isodensity, and prolonged enhancement of perinodular liver parenchyma was observed (Figs. 1J, 2F). On larger nodules, intra-tumoral normal portal vein and intra-tumoral hepatic artery were preserved without encasement on CTAP, representing preservation of the intra-tumoral portal tracts (Fig. 2D). SLD-CTHA provided further hemodynamic information (Fig. 2G). On SLD-CTHA, the nodule and perinodular liver parenchyma were gradually enhanced about 10–15 s after the start of contrast medium injection. Then the enhancement of the nodules gradually diminished from 30 to 35 s after the start of contrast medium injection, and prolonged enhancement of the perinodular liver parenchyma was observed until the end of the scanning.

Pathological features

On histopathological examination, macroscopically, all of the surgically resected lesions showed round and well-circumscribed nodules and were well demarcated from the surrounding liver parenchyma (Fig. 3A). Microscopically, the nodules consisted of marked lymphoid follicles and germinal centers without significant atypia on hematoxylin and eosin (HE) staining and were diagnosed as pseudolymphoma (Fig. 3B). Interestingly, in all cases, stenosis or disappearance of the portal venules, caused by marked lymphoid cell infiltration in the portal tracts, was observed in the perinodular liver parenchyma (Fig. 3C, D). These findings were observed only in the portal tracts just around the nodules, not in the portal tracts distant from them. The distribution of these lymphoid cell infiltrated portal tracts was almost identical with the area of perinodular enhancement observed on the CTHA images.

Five nodules, which were confirmed using percutaneous core needle biopsy specimen, exhibited similar microscopic findings, and three of them showed marked lymphoid cell infiltration in the portal tracts in background liver near the nodule.

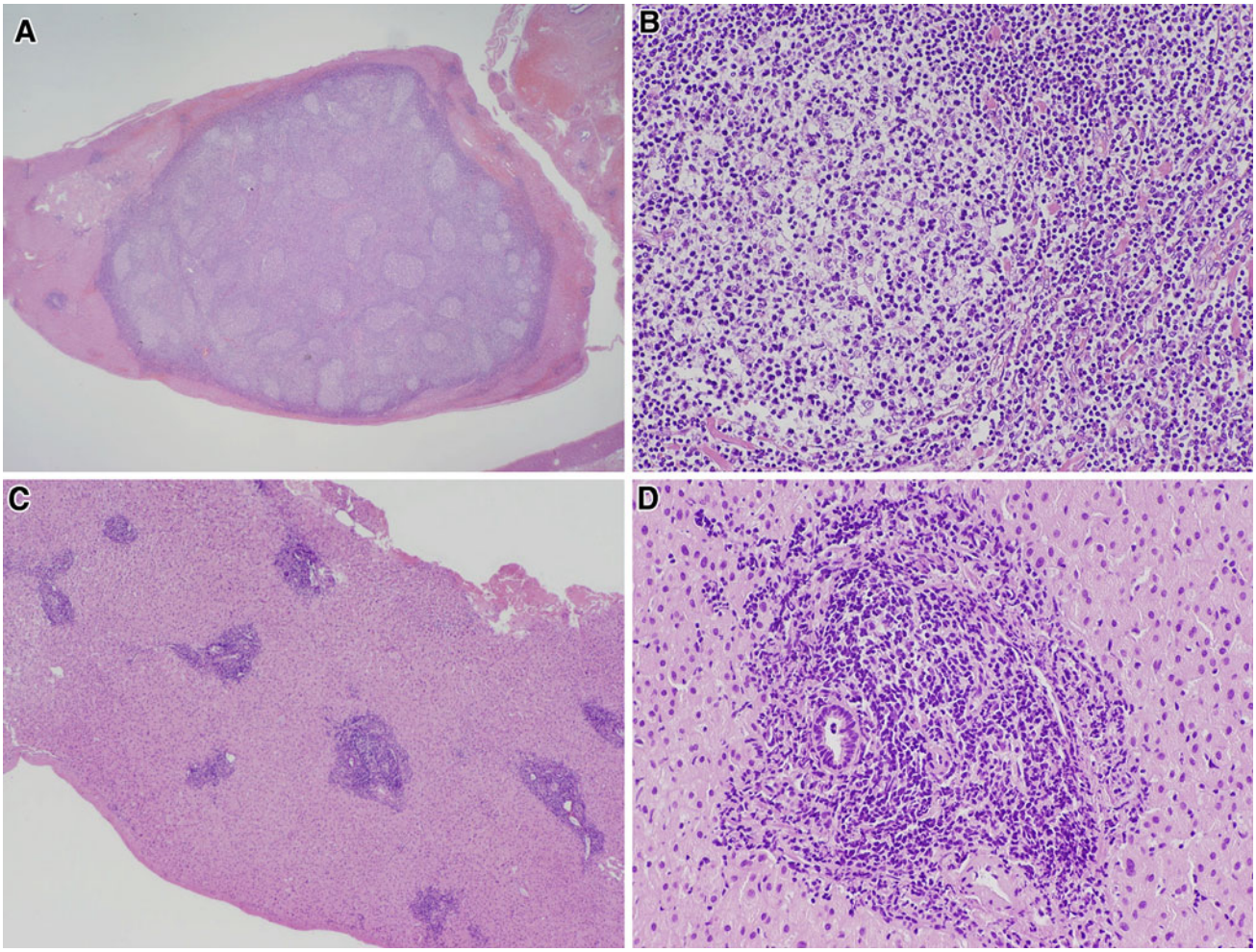

Fig. 3. A 43-year-old woman with pseudolymphomas of the liver in hepatic segment III and VI (patient 3). **A** Macrograph of resected specimen in hepatic segment VI shows round and well-circumscribed tumor (HE stain ×20). **B** The nodule consisted of marked lymphoid follicles and germinal centers without significant atypia (HE stain ×400). **C** Macrograph in the peritumoral area shows marked lymphoid cell infiltration within portal tracts was observed (HE stain ×80). **D** In the portal tract, disappearance of portal vein or oppressed portal venules were observed (HE stain ×400).

Follow-up data

The five pseudolymphomas confirmed with biopsy specimens were diminished or regressed on follow-up CT examinations without any treatment. No apparent recurrence or increase in the size of the nodules was observed in any patients including five operated cases.

Discussion

Hepatic pseudolymphoma had previously been thought be an extremely rare nodular lesion. However, recent advances in imaging modalities have resulted in frequent detection of hepatic pseudolymphoma, and the number of reports of such cases has increased. A review of the English literature revealed more than 40 cases reported to date [9]. Except for one 15-year-old woman, all patients were adult, and 88% were female. Most reported cases are single in number, although multiple lesions have been also reported. A case with a number of lesions, like in our two cases, has been also reported [10]. Although the precise etiology of hepatic pseudolymphoma is still unknown, it might involve infections or autoimmune reactions. The relatively high prevalence of autoimmune disorders suggests that autoimmunity may be implicated.

Making a diagnosis of hepatic pseudolymphoma by radiological study is challenging. Most cases reported previously were case reports, and no multi-case study focusing on the radiological findings has been reported. According to the previous case reports, most nodules were hypoechoic on US, and some had a hyperechoic rim, though some nodules were undetectable because of the small tumor size or localization [11]. On CT, the nodules tended to show hypodensity on precontrast images, slight early enhancement in the arterial dominant phase, and hypo to isodensity in the equilibrium phase.

On MRI, the nodules revealed hypointensity on T1-weighted images, hyperintensity on T2-weighted images, hyperintensity on DWI, marked hyperintensity on T2-weighted images of SPIO-enhanced MRI, and hypointensity on T1-weighted images on the hepatobiliary phase of Gd-EOB-DTPA-enhanced MRI. 70% of cases showed a tumor stain on angiography. [4–6, 8, 10–14]. Although there are many case reports as noted above, these findings are not specific, making them less useful in the discrimination of pseudolymphoma from other hepatic tumors. Especially, these findings are first cousins to those of hepatocellular carcinoma (HCC), or metastatic carcinoma, and most cases have been misdiagnosed as these based on the radiological findings.

In our hepatic pseudolymphoma cases, US, MRI signal intensity findings were similar to those previously described. In contrast, there were some unique findings in our cases on multi-phasic contrast-enhanced CT and MRI examinations. First, the nodules showed a homogeneous parenchymal pattern without necrosis or calcification on both of the modalities. This finding was clearly identified in the large mass-forming type more than 25 mm in diameter. This reflects the intra-tumorous homogeneity. On contrast-enhanced CT/MRI, normal hepatic arteries are seen to penetrate the nodule without serration or encasement on arterial dominant phase images. On CTAP, intranodular portal vein was partially preserved in the nodule. This vessel-penetrating sign suggests partial preservation of intra-tumoral portal tracts, which is not characteristic of HCC or metastatic tumor. This sign was also previously reported in one case of hepatic pseudolymphoma [10]. Second, the multi-phasic contrast-enhanced CT and MRI findings included a new one, which is ''perinodular enhancement'' on the arterial dominant or equilibrium phase. Recent innovations in multi-phasic contrast-enhanced CT, MRI, and contrast-enhanced US have facilitated analysis of the hemodynamics of the liver, including hepatic parenchyma and liver tumors [15]. In addition to them, angiography-assisted CT including CTHA, CTAP, and SLD-CTHA are useful methods to evaluate the hemodynamics of hepatic tumors [16–19]. Differences in the hemodynamics of hepatic tumors including HCC, metastatic tumor, and focal nodular hyperplasia facilitate the making of a pre-surgical radiological diagnosis [20–23]. The finding, ''perinodular enhancement'' of hepatic pseudolymphoma, was observed in 56%/67% of cases in this study on the arterial dominant phase and 44%/33% of cases on the equilibrium phase on CT/MRI, respectively. CTHA clarified that the perinodular enhancement, which clearly appeared on the early phase images of CTHA, was prolonged even in the delayed phase. On SLD-CTHA, perinodular liver parenchyma and the nodule were gradually enhanced simultaneously. Then, prolonged enhancement of perinodular liver parenchyma was observed until the end of the scanning, while the degree of enhancement of the nodule gradually diminished. CTAP showed no portal perfusion in the area of perinodular enhancement. Histopathological study revealed stenosis and/or disappearance of portal venules caused by marked lymphoid cell infiltration in the portal tracts adjacent to hepatic pseudolymphoma, and these histopathological changes were compatible with the radiological manifestations. Zen et al. suggested that lymphocytic infiltration extending along portal tracts around nodules might be characteristic for hepatic pseudolymphoma, and other resected cases have revealed the same histopathological features [5, 7, 12]. The reason for the stenosis and/or disappearance of portal venules in the portal tracts adjacent to nodules is still unknown. In fact, we presumed that histopathological changes caused portal flow disturbances and increased hepatic arterial flow in the perinodular liver parenchyma, resulting in early perinodular enhancement of the perinodular liver parenchyma.

It is well known that hemodynamic changes in liver parenchyma, including the perinodular area, occur in many hepatic diseases. Segmental enhancement is one of the hemodynamic changes in liver parenchyma, observed on early phase images of multi-phasic contrast-enhanced CT, MRI, and CTHA. Portal vein compression and obstruction due to HCC, liver metastasis from pancreatic carcinoma, hepatic abscess, and intrahepatic cholangitis causes segmental enhancement, which reflects decreased portal flow and increased hepatic arterial blood flow due to tumor cell or inflammatory cell infiltration in the perinodular portal tract (Glisson's capsule) [24–27]. The same pathological and consequent hemodynamic changes could occur in focal perinodular areas in hepatic pseudolymphoma.

CTHA shows that enhancement of the perinodular liver parenchyma (''corona enhancement'') is also observed in hypervascular HCC [20]. Perinodular enhancement of hepatic pseudolymphoma mimics corona enhancement of HCC on the equilibrium phase of CT or MRI. Since the corona enhancement of HCC is a result of drainage flow from the tumor sinusoids to hepatic sinusoids of the surrounding liver parenchyma through portal venules in the fibrous capsule, it appears gradually in the late phase images of CTHA. In contrast, perinodular enhancement of hepatic pseudolymphoma is observed on the early phase images of CTHA and is prolonged in the late phase.

Similar to hepatic pseudolymphoma, perinodular parenchymal enhancement may also be observed in metastatic liver tumors [21]. In hypovascular liver metastasis from colon, perinodular enhancement becomes prominent on early phase images, due to changes in the hemodynamics of the liver around the metastatic tumors such as increased arterial–portal shunting noted from an analysis of the SLD-CTHA findings. In liver metastasis from colon cancer, however, early rim

enhancement is frequently observed in hypovascular cases as compared with cases of hypervascular metastasis, making it distinguishable from hepatic pseudolymphoma, which often appears hypervascular.

There are several limitations in our study. First, of our ten nodules, full investigation of the radiologic–pathologic correlation was possible in only the five resected nodules, while the remaining five nodules could not be subjected to region to region correlated analysis. However, the biopsy specimens showed similar histopathological findings in the tumor area in all nodules, as well as perinodular liver parenchyma in three cases. In addition, two cases with multiple lesions showed similar hemodynamic characteristics on CTHA. The second limitation is that mucosa-associated lymphoid tissue lymphoma (MALT lymphoma) might show radiological findings similar to those of pseudolymphoma. Pseudolymphoma is a benign lesion, histopathologically characterized by marked proliferation of non-neoplastic and polyclonal lymphocytes forming follicles with active germinal centers. On the other hand, MALT lymphoma is a tumorous lesion consisting of clonal B cell lymphoproliferation with germinal centers histopathologically. However, both lesions share a nearly identical morphological appearance on H–E staining, and only immunohistological and genetic analyses to ascertain whether infiltrating lymphocytes are monoclonal or polyclonal can differentiate pseudolymphoma from MALT lymphoma [1, 3, 28]. Namely, since the cellular and vascular structures of pseudolymphoma and MALT lymphoma show almost the same pattern, with currently available radiological imaging modalities, these two entities cannot be reliably distinguished.

In conclusion, hepatic pseudolymphoma shows characteristic findings, such as homogeneous parenchymal pattern, vessel-penetrating sign in larger nodules, and unique enhancement pattern on multi-phasic CT/MRI and angiography-assisted CT. The enhancement pattern, named perinodular enhancement, reflects increased arterial supply in perinodular hepatic parenchyma caused by portal venular stenosis and/or disappearance due to marked lymphoid cell infiltration in perinodular portal tracts. This hemodynamic pattern has not been reported in HCC or other hypervascular tumors, and therefore, it may be useful in the differential diagnosis of hepatic pseudolymphoma.

References

1. Sharifi S, Murphy M, Loda M, Pinkus GS, Khettry U (1999) Nodular lymphoid lesion of the liver: an immune-mediated disorder mimicking low-grade malignant lymphoma. Am J Surg Pathol 23:302–308
2. Katayanagi K, Terada T, Nakanuma Y, Ueno T (1994) A case of pseudolymphoma of the liver. Pathol Int 44:704–711
3. Willenbrock K, Kriener S, Oeschger S, Hansmann ML (2006) Nodular lymphoid lesion of the liver with simultaneous focal nodular hyperplasia and hemangioma: discrimination from primary hepatic MALT-type non-Hodgkin's lymphoma. Virchows Arch 448:223–227
4. Doi H, Horiike N, Hiraoka A, et al. (2008) Primary hepatic marginal zone B cell lymphoma of mucosa-associated lymphoid tissue type: case report and review of the literature. Int J Hematol 88:418–423
5. Park HS, Jang KY, Kim YK, Cho BH, Moon WS (2008) Histiocyte-rich reactive lymphoid hyperplasia of the liver: unusual morphologic features. J Korean Med Sci 23:156–160
6. Maehara N, Chijiiwa K, Makino I, et al. (2006) Segmentectomy for reactive lymphoid hyperplasia of the liver: report of a case. Surg Today 36:1019–1123
7. Zen Y, Fujii T, Nakanuma Y (2010) Hepatic pseudolymphoma: a clinicopathological study of five cases and review of the literature. Mod Pathol 23:244–250
8. Okada T, Mibayashi H, Hasatani K, et al. (2009) Pseudolymphoma of the liver associated with primary biliary cirrhosis: a case report and review of literature. World J Gastroenterol 15:4587–4592
9. Amer A, Mafeld S, Saeed D et al. (2012) Reactive lymphoid hyperplasia of the liver and pancreas. A report of two cases and a comprehensive review of the literature. Clin Res Hepatol Gastroenterol 36:71–80
10. Osame A, Fujimitsu R, Ida M, et al. (2011) Multinodular pseudolymphoma of the liver: computed tomography and magnetic resonance imaging findings. Jpn J Radiol 29:524–527
11. Matsumoto N, Ogawa M, Kawabata M, et al. (2007) Pseudolymphoma of the liver: sonographic findings and review of the literature. J Clin Ultrasound 35:284–288
12. Kobayashi A, Oda T, Fukunaga K, et al. (2011) MR imaging of reactive lymphoid hyperplasia of the liver. J Gastrointest Surg 15:1282–1285
13. Machida T, Takahashi T, Itoh T, et al. (2007) Reactive lymphoid hyperplasia of the liver: a case report and review of literature. World J Gastroenterol 13:5403–5407
14. Takahashi H, Sawai H, Matsuo Y, et al. (2006) Reactive lymphoid hyperplasia of the liver in a patient with colon cancer: report of two cases. BMC Gastroenterol 12:25
15. Itai Y, Matsui O (1997) Blood flow and liver imaging. Radiology 202:306–314
16. Hayashi M, Matsui O, Ueda K, et al. (1999) Correlation between the blood supply and grade of malignancy of hepatocellular nodules associated with liver cirrhosis: evaluation by CT during intraarterial injection of contrast medium. Am J Roentgenol 172:969–976
17. Matsui O, Ueda K, Kobayashi S, et al. (2002) Intra- and perinodular hemodynamics of hepatocellular carcinoma: CT observation during intra-arterial contrast injection. Abdom Imaging 27:147–156
18. Matsui O, Takashima T, Kadoya M, et al. (1985) Dynamic computed tomography during arterial portography: the most sensitive examination for small hepatocellular carcinomas. J Comput Assist Tomogr 9:19–24
19. Matsui O, Kadoya M, Kameyama T, et al. (1991) Benign and malignant nodules in cirrhotic livers: distinction based on blood supply. Radiology 178:493–497
20. Ueda K, Matsui O, Kawamori Y, et al. (1998) Hypervascular hepatocellular carcinoma: evaluation of hemodynamics with dynamic CT during hepatic arteriography. Radiology 206:161–166
21. Terayama N, Matsui O, Ueda K, et al. (2002) Peritumoral rim enhancement of liver metastasis: hemodynamics observed on single-level dynamic CT during hepatic arteriography and histopathologic correlation. J Comput Assist Tomogr 26:975–980
22. Miyayama S, Matsui O, Ueda K, et al. (2000) Hemodynamics of small hepatic focal nodular hyperplasia: evaluation with single-level dynamic CT during hepatic arterioography. Am J Roentgenol 174:1567–1569
23. Terayama N, Matsui O, Gabata T, et al. (2001) Accumulation of iodized oil within the nonneoplastic liver adjacent to hepatocellular carcinoma via the drainage routes of the tumor after transcatheter arterial embolization. Cardiovasc Intervent Radiol 24:383–387
24. Matsui O, Takashima T, Kadoya M, et al. (1984) Segmental staining on hepatic arteriography as a sign of intrahepatic portal vein obstruction. Radiology 152:601–606
25. Gabata T, Matsui O, Terayama N, Kobayashi S, Sanada J (2008) Imaging diagnosis of hepatic metastases of pancreatic carcinoma:

significance of transient wedge-shaped contrast enhancement mimicking arterioportal shunt. Abdom Imaging 33:437–443
26. Gabata T, Kadoya M, Matsui O (2001) Dynamic CT of hepatic abscess: significance of transient segmental enhancement. Am J Roentgenol 176:675–679
27. Arai K, Kawai K, Kohda W, Tatsu H, Matsui O (2003) Dynamic CT of acute cholangitis: early inhomogeneous enhancement of the liver. Am J Roentgenol 181:115–118
28. Travis WD, Galvin JR (2001) Non-neoplastic pulmonary lymphoid lesions. Thorax 56:964–991